JPPIPA 11(4) (2025)

Jurnal Penelitian Pendidikan IPA

http://jppipa.unram.ac.id/index.php/jppipa/index

Seismic Attenuation Characteristics in Sumba Island Based on Coda Wave Analysis

Ayu Puput Ariyanti[1*], Titi Anggono[2], Aditya Dwi Prasetio[2], Kartika Hajar Kirana[1]

[1]Department of Geophysics, Faculty of Mathematics and Natural Sciences, Universitas Padjadjaran, Jatinangor, Indonesia.
[2]Research Center for Geological Disaster, National Research and Innovation Agency (BRIN), Bandung, Indonesia.

Received: December 16, 2024
Revised: March 13, 2025
Accepted: April 25, 2025
Published: April 30, 2025

Corresponding Author:
Ayu Puput Ariyanti
ayuariyantii03@gmail.com

DOI: 10.29303/jppipa.v11i4.10870

Abstract: Coda wave data from four stations are to understand seismic attenuation on Sumba Island. Specifically, we estimate the quality factor at 1 Hz (Q_0) and its frequency dependence (η) across multiple window lengths (20–120 s) and frequency bands (1–7 Hz) using waveform data from 394 local earthquakes. The aim is to evaluate how these parameters reflect crustal heterogeneity and tectonic activity. Results show that Q_0 increases with window length, indicating that coda waves progressively sample deeper and more homogeneous layers, while high η values at shorter windows suggest significant near-surface heterogeneity. These findings highlight a depth-dependent variation in seismic attenuation and structural complexity. The study reveals spatial variability, with MELO station showing anomalously high Q_0 values, likely due to localized site conditions or deeper structural influences. Sumba's location within the tectonically active Sunda-Banda arc transition zone further supports these observations. The combination of low Q_0 and high η values confirms high tectonic activity, and the use of coda wave attenuation analysis offers a reliable, parameter-based framework for assessing seismic hazard potential in regions with complex geodynamics. This work fills a research gap by providing empirical data and interpretation for a previously underexplored area in eastern Indonesia.

Keywords: Attenuation; Coda wave; Seismic; Sumba island; Tectonic

Introduction

Earthquakes are natural hazard phenomena caused by the sudden release of energy stored within the Earth's crust. This energy release generates seismic waves that propagate through the Earth's interior and surface, causing ground shaking of varying intensities. After arriving at the Earth's surface, these vibrations can damage buildings and infrastructure, leading to material losses or even fatalities (Sunarjo et al., 2012). The movement of tectonic plates, volcanic activity, and human-induced processes such as reservoir-induced seismicity and underground explosions can trigger earthquakes. The impact of earthquakes is not only determined by the magnitude of energy released but also by how seismic waves propagate and dissipate as they travel through the Earth's medium.

Attenuation decreases the amplitude of seismic waves propagating through the Earth's medium and causes energy loss due to various physical mechanisms. Seismic attenuation can be caused by intrinsic absorption and wave scattering (Ma'hood et al., 2009). While intrinsic absorption refers to the transformation of seismic energy into heat, scattering results in the redistribution of energy due to the interaction of seismic waves with the medium's heterogeneities such as fractures, faults, or lithological contrasts. These heterogeneities may act as scatterers that redistribute seismic energy leading to amplitude decay. The occurrence of scattering depends on the ratio between the size of the heterogeneities and the wavelength, as

How to Cite:
Ariyanti, A. P., Anggono, T., Prasetio, A. D., & Kirana, K. H. (2025). Seismic Attenuation Characteristics in Sumba Island Based on Coda Wave Analysis. *Jurnal Penelitian Pendidikan IPA*, *11*(4), 952-963. https://doi.org/10.29303/jppipa.v11i4.10870

well as the distance the wave travels through the heterogeneous area (Sato & Fehler, 2009).

The process occurs due to reflection and transmission at layer boundaries, geometrical spreading, or seismic energy conversion into heat. Seismic attenuation estimates are derived from the decay of coda waves, which appear after S-waves at the end of seismic recording events and consist of incoherent waves scattered by subsurface inhomogeneities (Filippucci et al., 2021). Several studies showed that scattering attenuation can be significant in regions with complex structures, such as active fault zones or volcanic regions (Carcole & Sato, 2010; Havskov et al., 2016; Pezzo, 2008; Prudencio et al., 2017).

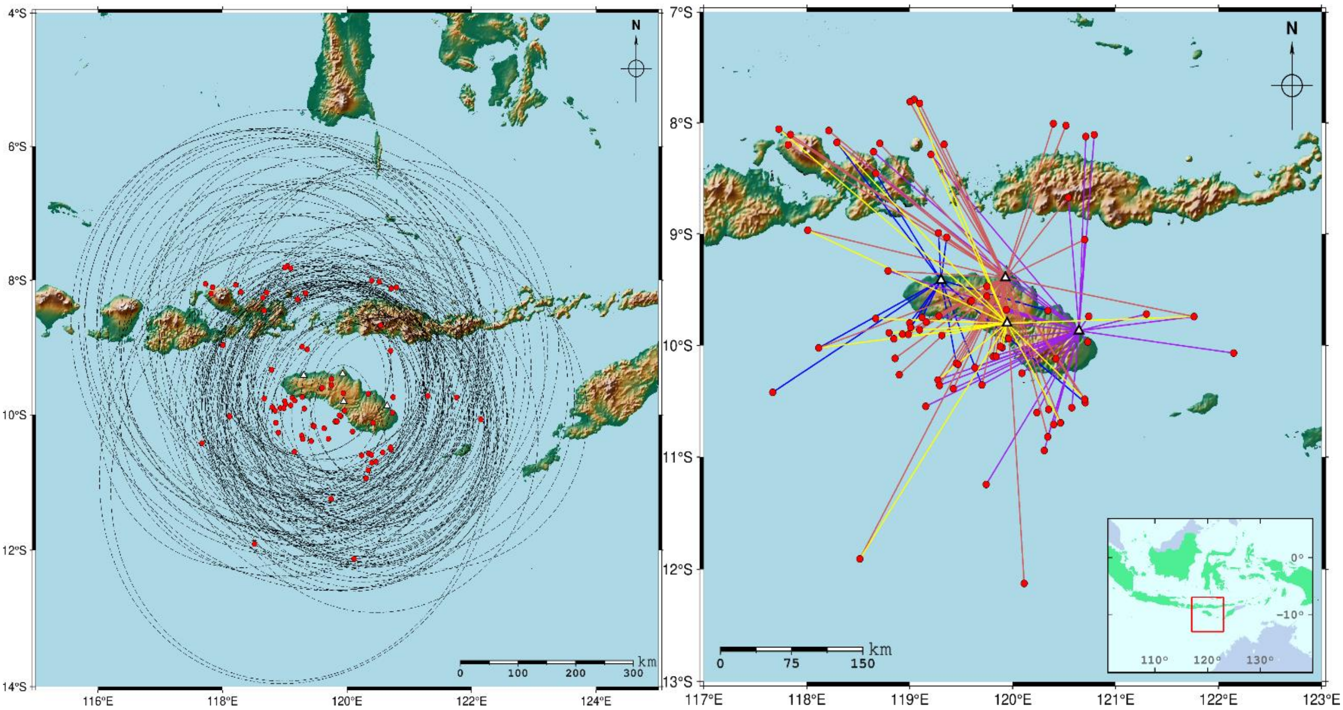

Figure 1. Distribution of earthquakes recorded at four stations: BULE, KPAR, MELO, and NAPU, using a window length of 60 seconds. The scattering ellipses (left) and the raypath of seismic wave propagation (right) are shown. Red circles indicate earthquake locations, whereas white triangles represent station locations.

Attenuation is characterized by the Quality factor (Q), which describes the ratio of energy retained in a propagating seismic wave to the energy lost per cycle, where higher Q values indicate lower energy attenuation (Sharma & Mitra, 2018; Wang & Shearer, 2017). A higher Q value suggests a more homogeneous medium that absorbs less seismic energy, whereas a lower Q value indicates a more heterogeneous medium that absorbs more energy. Studies across different tectonic settings have demonstrated this relationship between Q values and geological conditions (Havskov et al., 2016; Sharma & Mitra, 2018). For instance, stable continental crusts show high Q_c values (200–800), reflecting minimal attenuation due to their old, uniform structure (Mitchell, 1995; Singh et al., 2019). In contrast, active or complex regions such as the Zagros collision zone or volcanic arcs show significantly lower Q_c values, often below 100, due to increased faulting, fracturing, elevated temperatures, or the presence of fluids and magma (Talebi et al., 2024; Wu et al., 2006). These variations illustrate how Q can serve as a diagnostic parameter for subsurface complexity and seismic potential.

Aki & Chouet (1975) demonstrated that coda waves can be used to determine a specific quality factor known as Q_c. The amplitude of coda waves as a function of frequency and time for a local earthquake, at a lapse time (measured from the event origin) is given by Equation 1.

$$A(f,t) = S(f)t^{-\beta}e^{-\frac{\pi f t}{Q_c}} \quad (1)$$

where $A(f,t)$ represents the amplitude of the coda wave at time (t) and frequency (f). The function $S(f)$ represents the coda source factor, which depends on frequency but remains independent of time and radiation patterns, making it a constant for a specific narrow frequency band (Dasović et al., 2012). The parameters β and Q_c correspond to the geometrical spreading factor and the coda quality factor, respectively, where β is typically taken as 1 for body-wave scattering (Jin & Aki, 1988; Sato & Fehler, 1998). The frequency dependence of Q_c is written as on Equation 2.

$$Q_c = Q_0\left(\frac{f}{f_0}\right)^n \quad (2)$$

Q_0 represents the quality factor (Q_c) at a reference frequency f_0 (typically 1 Hz) and η denotes the frequency dependency (Hwang & Mitchell, 1987). The parameters $Q_0$and η provide essential insights into the seismic properties of a region. Q_0, which represents the reference quality factor, is influenced by factors such as tectonic setup, subsurface medium, and the degree of fracturing (Singh et al., 2019). Low Q_0 values typically indicate more heterogeneous regions with higher seismic energy dissipation. The correlation between $Q_0$and η has also been carried out by other studies which indicate that active tectonic regions tend to have higher η values and lower Q_0 values (Aki, 1980a, 1980b; Jin & Aki, 1988; Roecker et al., 1982; Singh & Herrmann, 1983). In this way, the results obtained will be useful for scenario hazard assessment of the area.

Building on these theoretical foundations, this study applies coda wave analysis to examine seismic attenuation in a geologically complex region: Sumba Island. Sumba is located in East Nusa Tenggara, Indonesia, within a highly active seismic zone influenced by the interaction of the Indo-Australian and Eurasian plates. Tectonically, Sumba occupies a forearc position within the Australian-Indonesian convergent margin, representing a sliver of arc crust that has been displaced from its original position (Keep et al., 2003). This tectonic setting is very complex, as it represents a transition from subduction along the Sunda arc to collision in the Banda arc (Syuhada et al., 2020). In the western region of Sumba, the Indo-Australian plate subducts beneath the Eurasian plate at a rate of approximately 70 mm/year in a N13E direction, gradually slowing to around 15 mm/year near the Timor Trough as it moves eastward (Bock et al., 2003; Curray, 1989).

Although plate convergence rates differ across the region, their connection to seismic activity is complex and non-linear. The variation in convergence rates (from ~70 mm/year in western Sumba to ~15 mm/year near the Timor Trough) contributes to differential stress accumulation across the region. Regions with higher convergence rates may accumulate more stress, potentially generating larger but less frequent earthquakes in the western part of the island, while areas with slower convergence might experience more frequent but lower-magnitude seismic events (McCaffrey, 2009). Nonetheless, the pattern of seismicity is also shaped by other crucial factors such as variations in coupling coefficient, fault geometry, rheological properties of the lithosphere, and pre-existing structural discontinuities. Particularly, the transition from oceanic to continental subduction along the Sunda-Banda arc boundary, where Sumba is located, generates a complex stress field that cannot be explained by convergence rates alone. This complexity makes Sumba Island an important location for studying how variations in plate boundary characteristics affect seismic energy propagation and attenuation.

This complex tectonic framework not only influences the dynamics of plate convergence, but also governs the structural deformation expressed across the island. Sumba lies at the transition zone between oceanic and continental lithosphere subduction, where tectonic forces have resulted in significant upper-plate deformation. The island is currently undergoing dextral en-échelon folding, and offshore to the west, focal mechanisms reveal active reverse and strike-slip faulting that defines a dextral transpressional zone. These structures reflect strong shear stress transfer from the subducting Indo-Australian plate to the overriding Eurasian plate, a process favored by strong interplate coupling. The uplift of Sumba and lateral shearing of the accretionary prism are attributed to the Plio-Quaternary subduction of the western edge of the Australian continental margin. Together, these tectonic features contribute to the active seismicity in the region and illustrate the complex deformation patterns arising at the transition from oceanic to continental subduction (Authemayou et al., 2022). The presence of intense faulting, structural complexity, and lateral variations in crustal properties makes Sumba Island a compelling natural laboratory for investigating coda wave attenuation. The heterogeneity of the upper crust associated with this tectonic complexity enhances seismic wave scattering, which is precisely the behavior that coda wave analysis is designed to capture.

Research on seismic attenuation in Indonesia remains relatively scarce, despite the country's high level of seismicity and its complex tectonic setting. Previous research has primarily focused on isolated volcanic regions or specific high-risk areas. For instance, Priyono et al. (2011) conducted a three-dimensional seismic attenuation study of Mt. Guntur in West Java, while more recently, Priyono et al. (2021) performed seismic attenuation tomography following the 2018 Lombok earthquakes. However, comprehensive attenuation studies across the Indonesian archipelago remain sparse, with a notable absence of research specifically addressing the Sumba Island region. This research gap is particularly significant given Sumba's unique position within the transition zone between the Sunda and Banda arcs, where changes in subduction dynamics could substantially influence seismic wave propagation and attenuation patterns. In light of this, the present study investigates seismic wave attenuation, with a specific focus on coda wave attenuation estimates using data from four different stations for a tectonic analysis of the region (Figure 1). Analyzing coda waves can provide crucial insights into the scattering and attenuation processes within the subsurface, helping to characterize the region's seismic properties.

This study represents the first comprehensive analysis of coda wave attenuation in Sumba Island, a region of significant tectonic complexity that has received limited attention in seismic attenuation studies despite its unique position at the Sunda-Banda transition zone. Previous seismic investigations in this region have primarily focused on velocity tomography and earthquake distribution. In contrast, our research fills a critical knowledge gap by characterizing the seismic attenuation properties specifically in Sumba Island using data from multiple stations. The novelty of this work lies in its integration of quality factor analysis across varying window lengths and frequencies to develop a three-dimensional understanding of subsurface heterogeneity in this transitional tectonic setting. The findings may contribute significantly to regional seismic hazard assessment by providing quantitative parameters (Q_0 and η values) that can be incorporated into ground motion prediction equations and seismic hazard models. Additionally, this research advances our fundamental understanding of how complex tectonic transitions affect seismic wave propagation characteristics, with implications for similar tectonic settings globally.

Method

This study employs earthquake waveform data in the Seismic Analysis Code (SAC) format from seismic project: Transitions in the Banda Arc-Australia continental collision which recording the seismic activity along Banda Arc temporarily between 2014-2016 (Miller, 2019). AusPass provided the data: Australian Passive Seismic Server with network code of YS. Four seismic stations were deployed on Sumba Island, namely BULE, KPAR, MELO, and NAPU, with a sampling rate of 50 Hz. The sensors used are Streckeisen STS-2 G3 with Quanterra 330 data logger, which record three components (BH1, BH2, BHZ).

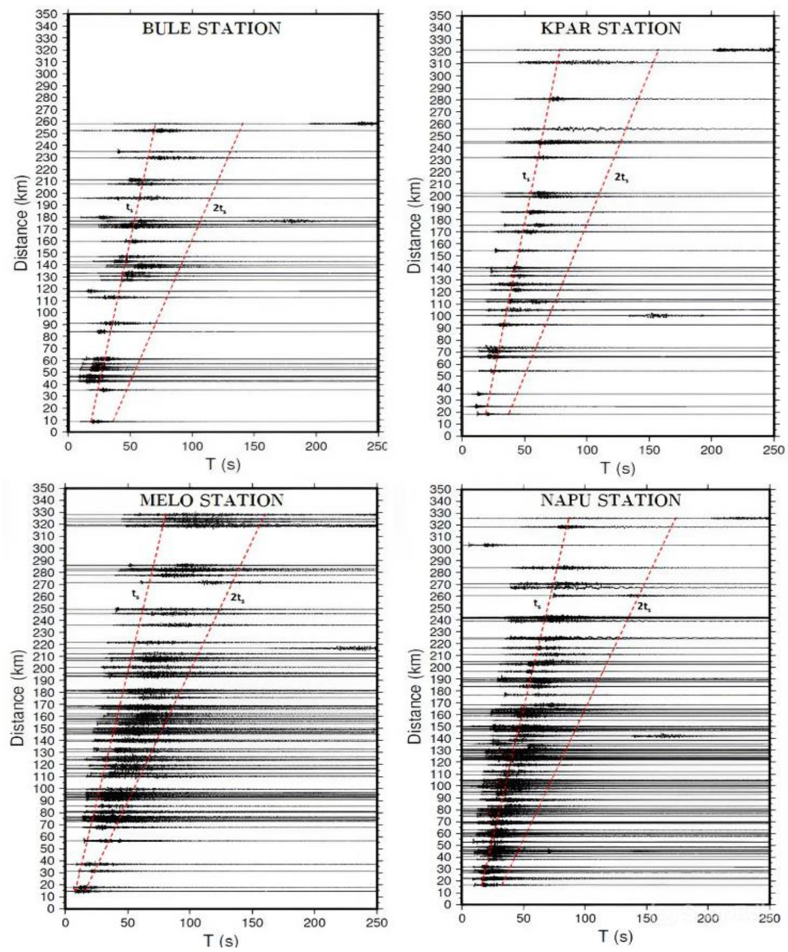

Figure 2. Recorded waveforms at BULE, KPAR, MELO, and NAPU stations. The red dashed lines, marked as ts and 2ts, indicate the estimated arrival times of the S-wave and coda wave.

The coda attenuation analysis requires a local earthquake event with epicentral distance less than 350 km and depth less than 40 km. The earthquake event was searched from the International Seismological Center (ISC) catalog for magnitudes ranging from 3 to 6, and 1136 events were found. The shallow earthquake is chosen because the coda wave mechanism should come from the scattering wave on the earth's crust, assuming the average crust depth is 40 km. The coda wave amplitude decay from distinct earthquakes depends on the lapse time from origin time but is independent of distance. In addition, the amplitude decay also does not depend on the magnitude of earthquakes with a magnitude of less than 6 (Aki, 1969; Aki & Chouet, 1975). Early data selection is done by inspecting each waveform, especially the vertical component (BHZ) used in the calculation. The process plots the waveform to ensure it fully records the event without missing data. The main criteria are that the P and S wave arrivals are distinguishable. Instrument correction was applied to remove the bias and distortion caused by the sensor frequency response and sensitivity. This ensured that the data represented actual ground motion without instrument affection, and the data value was converted from count/second into velocity (m/s). P and S waves' arrival times were manually picked for each waveform. This step is essential for calculating the signal-to-noise ratio and determining the coda start time. The noise portion is 10 seconds before P arrival, and the signal part of the coda wave is twice the arrival of the S wave. The coda waveform segment, starting at 2ts, and the vertical component analysis for a 60-second window are illustrated in Figure 2.

The only waveforms with an SNR greater than five were selected in this study. A total of 394 waveforms of vertical components fulfills the requirement for coda attenuation analysis. The essential step before calculating coda attenuation is separating the data into several frequency bands. All waveforms are filtered by a four-pole Butterworth filter with a central frequency of 1, 1.5, 2, 3, 4, 5, 6, and 7 Hz, which is determined based on the Nyquist frequency. This filtering process assures that the analysis captures the frequency-dependent characteristics of coda wave attenuation. By dividing the data into narrow frequency bands, we can more accurately identify and isolate the coda waves. The calculations were performed based on coda wave data for each window lengths, ensuring a comprehensive frequency-dependent Q_c estimation.

Each frequency band is centered around a specific frequency, and the data within that band is filtered to retain only the components falling within 1/3 of the central frequency range. This approach allows for a detailed examination of how coda wave attenuation varies across different frequencies, providing insight into the frequency-dependent behavior of seismic waves.

Based on the empirical approach by Aki & Chouet (1975), the root-mean-square amplitude $A(f|t)$, which is manually drawn and smoothed, is roughly two times the power spectral density $P(f|t)$ and the bandwidth is expressed as:

$$A(f|t) = 2[2P(f|t)\Delta f]^{1/2} \quad (3)$$

Later, this equation's power spectra density term is substituted from the diffusion theory, resulting in Equation (1).

The parameters β and Q_c correspond to the geometrical spreading constant, 0.5 for surface waves and 1 for body waves, and the coda quality factor, respectively. β is a taken as one since the coda wave results from the scattering of the body, dominantly S wave (Jin & Aki, 1988; Sato & Fehler, 1998). The process of estimating the Q_c is done by taking the natural logarithm of eq (1) to linearize the equation:

$$\ln A(f,t) = \ln S(f) - \beta \ln(t) - bt \quad (4)$$

by fitting a linear regression line to $ln(A(f, t))$ vs t, we can calculate Q_c from the slope b as:

$$Q_c = \frac{-\pi f}{b} \quad (5)$$

The envelope of the coda as a function of time theoretically does not depend on the source factor. So, for two nearby events recorded in the same station, assuming that the time-dependent variable is the same for both events, the ratio of coda amplitude is equal to the ratio of coda source factor. Likewise, the source factor in Equation (4) can be disregard.

This calculation of the Q_c method assumes that the coda waves are backscattered from the region around the earthquake hypocenter and station location in an elipsoidal halfspace (Sato, 1977). The 2 dimension geometry is reduced by replacing the hypocenter with the earthquake's epicenter, and this simplification is valid for local earthquakes with shallow depth (Sharma & Mitra, 2018). The elliptical shape depends on epicentral distance (R) and the maximum coda lapse time (T_{max}). The lateral resolution of coda Q is influenced by the T_{max}, which larger the time means the coda waves sampled a larger area. Based on Pulli (1984), the length of the ellipse semimajor axis calculated by $a_1 = V_s t_{max}/2$ and the semiminor axis $a_2 = \sqrt{a_1 - (R/2)^2}$. Where V_s is the mean S wave velocity, which is taken at 3.5 km/sec.

Alongside with the calculation of Q_c^{-1}, the Q_c at reference frequency (f_0 = 1 hz) denotes as Q_0 also estimated. The estimation of Q_0 express by Hwang & Mitchell (1987) as:

$$Q_c = Q_0 \left(\frac{f}{f_0}\right)^{\eta} \quad f_0 = 1 \quad (6)$$

$$\ln(Q_c) = ln(Q_0) + \eta \, ln(f) \quad (7)$$

the η represents the frequency dependency of coda Q, then by taking the natural logarithm of equation (6) the $ln(Q_0)$ is obtained from the intercept and slope (η). The values of Q_0 and η were determined using each window lengths ranging from 20 to 120 seconds, with an increment of 5 seconds. The selection of the maximum window length for coda wave analysis depends on the decay rate of coda energy for each earthquake event. A 5-second increment was applied to monitor the trend and changes in Q_0 values with increasing sampling time. The entire dataset was selected based on an epicentral distance range of 0–350 km. Finally, the obtained values of Q_0, Q_c, and η were analyzed to examine their relationship with the tectonic dynamics of the study area. The earthquake data processing workflow is illustrated in Figure 3.

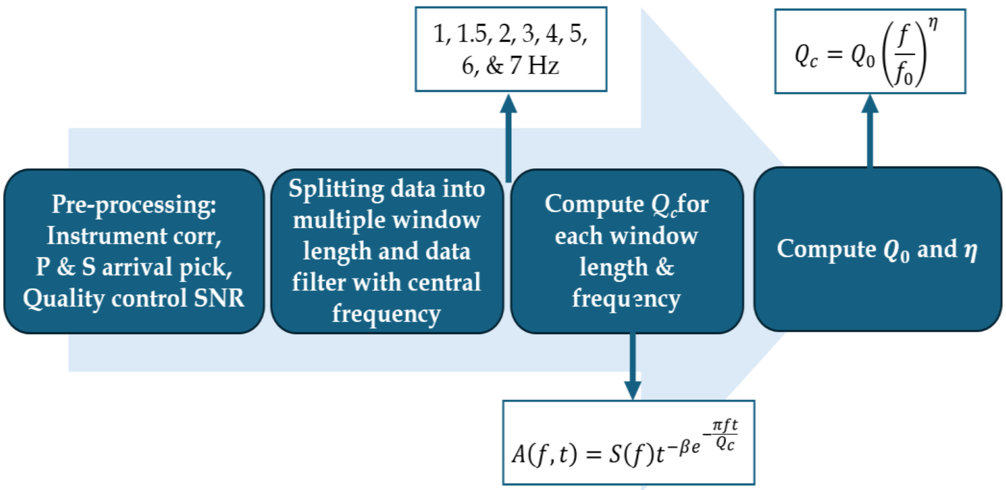

Figure 3. The flowchart of this research

Result and Discussion

The study of coda wave attenuation from seismic data recorded at multiple stations reveals that Q_0 increases with increasing window length. The scattering ellipse represents volume where coda sampling the medium (Figure 1). Based on Table 1, the Q_0 values at all stations remain below 200, with relatively high η values, indicating that the study area exhibits tectonically active characteristics. Figure 4 further supports this interpretation by showing a dense distribution of shallow to intermediate-depth earthquakes along the southern margin of Sumba Island, consistent with the activity of an underlying subduction zone. The spatial pattern of seismicity aligns well with the tectonic framework inferred from the Q_0 and η characteristics. This finding aligns with previous studies, which suggest that low Q_0 values (< 200) are commonly found in regions with high tectonic activity. In contrast, higher Q_0 values (> 600) are associated with stable tectonic regions (Mak et al., 2004). Furthermore, previous studies have also shown that η values tend to be higher in tectonically active regions, reflecting greater structural heterogeneity and elevated seismic activity (Aki, 1980a, 1980b; Roecker et al., 1982).

Table 1. Recapitulation of the results of coda wave attenuation calculations at the recording station

	Window length (s)	Q_0 ± std	η ± std
BULE	20	51.32 ± 7.71	1.22 ± 0.07
	40	130.64 ± 14.91	0.90 ± 0.05
	60	148.74 ± 6.93	0.86 ± 0.02
	80	161.98 ± 6.75	0.81 ± 0.02
	100	161.43 ± 4.96	0.84 ± 0.03
	120	160.66 ± 4.15	0.90 ± 0.03
MELO	20	100.91 ± 9.39	0.83 ± 0.08
	40	159.23 ± 9.28	0.78 ± 0.05
	60	181.25 ± 7.11	0.79 ± 0.04
	80	206.75 ± 8.47	0.79 ± 0.04
	100	215.93 ± 8.49	0.85 ± 0.04
	120	231.39 ± 9.38	0.90 ± 0.03
KPAR	20	95.56 ± 25.95	0.94 ± 0.10
	40	126.28 ± 10.82	0.91 ± 0.07
	60	149.78 ± 13.09	0.84 ± 0.05
	80	160.07 ± 11.62	0.80 ± 0.03
	100	158.09 ± 8.31	0.86 ± 0.04
	120	162.29 ± 5.55	0.95 ± 0.06
NAPU	20	96.44 ± 13.46	0.92 ± 0.06
	40	136.47 ± 6.82	0.85 ± 0.02
	60	154.57 ± 5.10	0.82 ± 0.02
	80	169.33 ± 4.40	0.81 ± 0.02
	100	174.34 ± 3.66	0.84 ± 0.02
	120	179.32 ± 2.90	0.87 ± 0.02

At the BULE station, Q_0 increases from 51.33 ± 7.71 at 20 s to 160.66 ± 4.15 at 120 s, indicating that coda waves sample deeper medium layers as the window length increases. A similar trend is observed at the MELO station, where Q_0 increases from 100.91 ± 9.39 at 20 s to 231.39 ± 9.38 at 120 s. The other stations, KPAR and NAPU, show a consistent increase, with Q_0 reaching 162.29 ± 5.55 and 179.32 ± 2.91 at 120 s, respectively. In addition to Q_0, the η values also exhibit significant variation across different stations. At BULE, η decreases from 1.221 ± 0.0717 at 20 s to 0.9023 ± 0.0384 at 120 s, indicating that the sampled medium becomes more homogeneous at longer window lengths. In contrast, at MELO, η increases slightly from 0.8325 ± 0.0841 to 0.9002 ± 0.0366 over the same window length interval. Similar trends are observed at KPAR (0.9449 ± 0.1042 to 0.9561 ± 0.0613) and NAPU (0.9249 ± 0.0645 to 0.8777 ± 0.0233), reflecting differences in the degree of subsurface heterogeneity across stations. These differences in η values likely reflect spatial variations in tectonic deformation, lithological heterogeneity, and crustal fracturing across the study area. Previous studies have similarly reported that Q_0 and η are influenced by factors such as tectonic setup, subsurface medium properties, and seismicity levels (Aggarwal & Khan, 2016; Jin & Aki, 1989; Mitchell, 1995; Rahimi et al., 2010; Rahimi & Hamzehloo, 2008; Singh et al., 2001).

The x-axis of Figure 5 represents the coda wave window length (in seconds), while the y-axis shows the corresponding values of Q_0 and η. The trends observed in Figure 5 support the interpretation of the results by showing a consistent increase in Q_0 and associated variations in η with increasing window length. At shorter window lengths (20–50 seconds), Q_0 increases rapidly and η varies significantly, indicating that coda waves are sampling shallower, more heterogeneous structures. Beyond 50 seconds, the trends of Q_0 and η become relatively stable, suggesting that coda waves progressively interact with deeper, more homogeneous layers where scattering and attenuation are reduced. This indicates that coda waves in longer window lengths propagate through a larger portion of the lithosphere, including the lower crust and upper mantle (Singh et al., 2019). This interpretation is further supported by previous studies, which have shown that coda waves at longer lapse times reflect the propagation of backscattered body waves through the more homogeneous lower crust and upper mantle (Kumar et al., 2005; Parvez et al., 2008; Woodgold, 1994; Zelt et al., 1999). This finding supports the hypothesis that regions with high tectonic activity tend to have lower Q_0 values and higher η values than more stable areas (Jin & Aki, 1988; Singh & Herrmann, 1983).

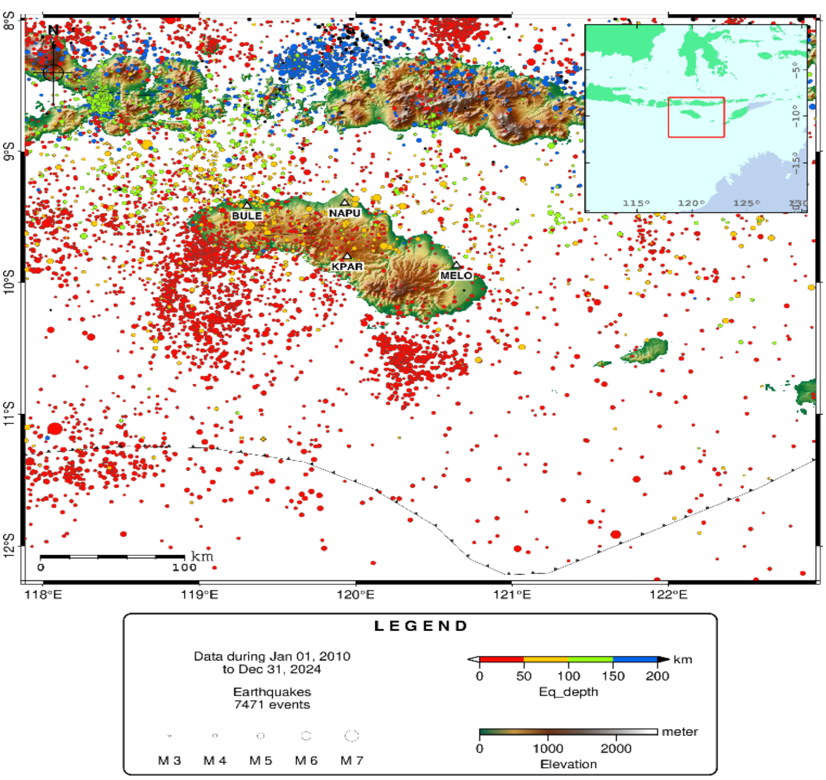

Figure 4. Epicenter distribution earthquakes around Sumba Island from 2010 to 2024, color-coded by earthquake depth. The size of each circle corresponds to earthquake magnitude (M3–M7). White triangles indicate the locations of seismic stations BULE, NAPU, KPAR, and MELO. The dense seismicity reflects active subduction along the southern boundary of the island. Inset shows the regional location of Sumba Island within eastern Indonesia.

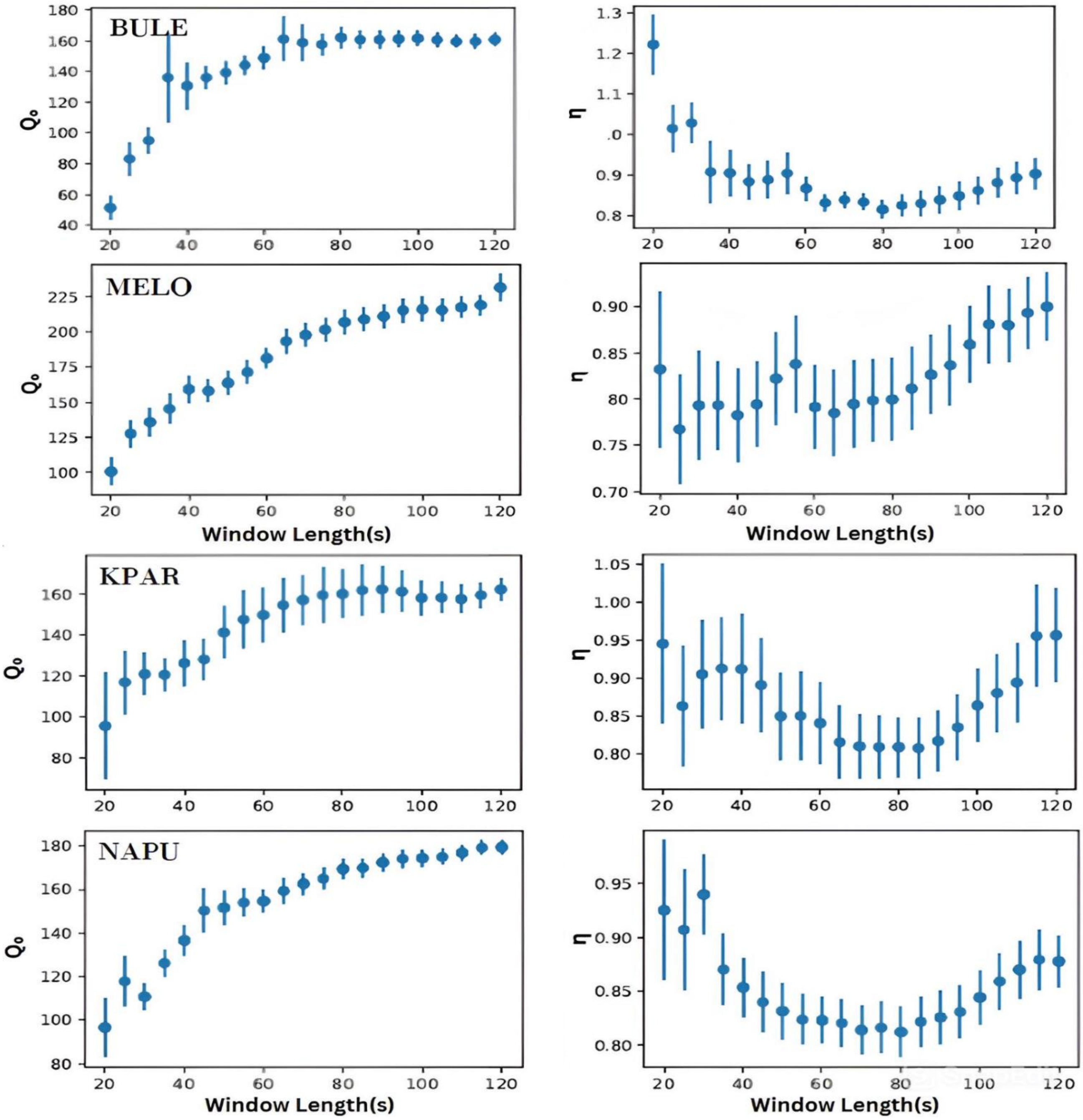

Figure 5. Q_0 and η as a function of window length calculated at an epicentral distance of 0–350 km.

The analysis of coda attenuation (Q_0) across four stations on Sumba Island (NAPU, BULE, KPAR, and MELO) reveals a notable anomaly: MELO, situated on Quaternary sediments (Authemayou et al., 2022), exhibits a relatively higher Q_0 compared to the other stations (BULE and KPAR) located on Tertiary sediments (Authemayou et al., 2022). This observation contradicts the general expectation that younger, less consolidated Quaternary sediments typically exhibit higher attenuation than older, more lithified Tertiary sediments. While the surface geology suggests higher attenuation at MELO and NAPU due to potential higher porosity and fluid content in the younger sediments, the higher Q_0 at MELO implies a locally less attenuating environment, possibly due to specific properties of the Quaternary sediments there (e.g., being well-drained or thin) or the influence of deeper structures.

Further complicating this picture is the finding from receiver function studies indicating a low-velocity zone (LVZ) beneath the MELO station (Syuhada et al., 2016). LVZs are typically associated with higher attenuation. The fact that MELO shows higher Q_0 despite this underlying LVZ suggests that the coda waves analyzed might not be strongly influenced by this deeper attenuating zone, possibly due to its depth or localized scattering characteristics. Alternatively, the near-surface conditions at MELO might contribute to a lower overall attenuation of the scattered waves. The variability in Q_0 across Sumba likely reflects a complex interplay of surface geology (Authemayou et al., 2022), local tectonic deformation related to the active subduction zone, and deeper velocity/attenuation structures like the LVZ beneath MELO (Syuhada et al., 2016), highlighting the need for integrated geophysical studies to understand seismic wave propagation on the island entirely. This pattern is consistent with the tectonic setting of the Sunda-Banda arc transition, where active subduction and oblique collision contribute to crustal deformation and fragmentation. These tectonic processes increase lithological heterogeneity and fracturing in the upper crust, which are known to enhance seismic attenuation and lead to lower Q_0 and higher η values in shallow layers.

Besides window length, epicentral distance also influences coda wave propagation by affecting the depth of sampled structures. Greater distances allow coda waves to interact with deeper, more stable geological layers with lower attenuation. Higher η values indicate propagation through heterogeneous media at shorter window lengths, while higher Q_0 values reflect sampling of deeper, more homogeneous structures at longer windows. Further analysis shows that, for a fixed window length, Q_0 and η exhibit no systematic variation with epicentral distance, consistent with Sharma & Mitra (2018), which suggested that this behavior is possibly a result of averaging across different tectonic units with varying Qc values sampled by single-trace measurements. In contrast, increasing the window length at a given distance consistently results in rising Q_0 and decreasing η values, which is attributed to deeper sampling volumes enabled by longer coda windows, where seismic attenuation diminishes as the Earth's structure becomes more homogeneous. As depth increases, intrinsic attenuation becomes less significant, leading to higher quality factors and reduced frequency dependence. While both epicentral distance and window length influence the sampling of Earth's interior, the variations observed in Q_0 and η in this study appear more strongly associated with changes in window length, consistent with the depth-dependent coda wave behavior reported by Sharma & Mitra (2018).

These attenuation patterns not only reflect general seismic propagation behavior but also offer important insights into the tectonic characteristics of the study area. The Q_0 and η characteristics derived from coda wave attenuation analysis in Sumba Island, East Nusa Tenggara, Indonesia, reflect a complex tectonic setting due to its location within the Sunda-Banda transition zone. This region lies at the boundary between the Eurasian and Indo-Australian Plates, which undergoes active convergence, subduction, and collisional tectonics. The low Q_0 values (< 200) and relatively high η values at shorter window lengths indicate that the subsurface medium in this region exhibits high heterogeneity and significant wave attenuation, typical of areas experiencing intense tectonic deformation. Moreover, the increase in Q_0 at longer window lengths suggests that coda waves persisting for extended periods sample deeper, more homogeneous, and mechanically stable layers, likely extending into the lower crust and upper mantle.

Conclusion

This study demonstrates that coda wave attenuation analysis is valuable for identifying whether a region is tectonically active or stable, based on Q_0 and η values. The results indicate that Sumba Island is an active tectonic region, as evidenced by its average Q_0 values below 200, suggesting a high susceptibility to tectonic hazards. In contrast, higher η values reflect greater medium heterogeneity of the earth's crust. Furthermore, tectonic events occurring in the Banda Arc region are likely to influence the tectonic dynamics of Sumba Island, further contributing to its seismic vulnerability. Calculations in this study were conducted at four seismic stations: BULE, NAPU, KPAR, and MELO, with the MELO station exhibiting a higher quality factor (Q) than the others, indicating lower seismic wave attenuation in that area. This suggests that seismic energy is better preserved at MELO, making it less attenuated than other regions. Our findings on Sumba Island show a surprising result about how seismic waves are attenuated. At a location with young, soft ground (MELO), the waves faded less than with older, harder ground. This is not what we usually expect, as soft ground typically causes waves to lose energy more quickly. Additionally, a study found a slow zone deep beneath MELO, which should also lead to faster wave weakening. This suggests that the underground conditions significantly affect how earthquake waves travel, more so than just the type of ground we see at the surface. Therefore, to better predict how strong earthquake shaking will be in different parts of Sumba, we must consider both the surface geology and the deeper structures within the crust.

Acknowledgments

Seismic data were obtained from the GEOFON data centre of the GFZ German Research Centre for Geosciences. Several pictures and maps were generated by the Generic Mapping Tools program.

Author Contributions

Conceptualization, methodology, software, validation, formal analysis, A.P.A., T.A., and A.D.P.; investigation, resources, data curation, writing—original draft preparation, visualization, project administration, A.P.A.; writing—review and editing, A.P.A., T.A., A.D.P., and K.H.K.; supervision, T.A., A.D.P., and K.H.K.; funding acquisition, T.A. All authors have read and agreed to the published version of the manuscript.

Funding

This study was supported by Rumah Program Kebencanaan – Research Organization of Earth Sciences and Maritime (National Research and Innovation Agency) No SP DIPA-124.01.1.690501/2024.

Conflicts of Interest

The authors declare no conflict of interest regarding the publication of this paper.

References

Aggarwal, S. K., & Khan, P. K. (2016). Q Lg Tomography in Gujarat, Western India. *Physics and Chemistry of the Earth, Parts A/B/C*, *95*, 135–149. https://doi.org/10.1016/j.pce.2015.12.003

Aki, K. (1969). Analysis of the Seismic Coda of Local Earthquakes as Scattered Waves. *Journal of Geophysical Research*, *74*(2), 615–631. https://doi.org/10.1029/JB074i002p00615

Aki, K. (1980a). Attenuation of Shear-Waves in the Lithosphere for Frequencies from 0.05 to 25 Hz. *Physics of the Earth and Planetary Interiors*, *21*(1), 50–60. https://doi.org/10.1016/0031-9201(80)90019-9

Aki, K. (1980b). Scattering and Attenuation of Shear Waves in the Lithosphere. *Journal of Geophysical Research: Solid Earth*, *85*(B11), 6496–6504. https://doi.org/10.1029/JB085iB11p06496

Aki, K., & Chouet, B. (1975). Origin of Coda Waves: Source, Attenuation, and Scattering Effects. *Journal of Geophysical Research*, *80*(23), 3322–3342. https://doi.org/10.1029/JB080i023p03322

Authemayou, C., Pedoja, K., Chauveau, D., Husson, L., Brocard, G., Delcaillau, B., Perrot, J., Aribowo, S., Cahyarini, S. Y., Elliot, M., Natawidjaja, D. H., & Scholz, D. (2022). Deformation and Uplift at the Transition from Oceanic to Continental Subduction, Sumba Island, Indonesia. *Journal of Asian Earth Sciences*, *236*, 105316. https://doi.org/10.1016/j.jseaes.2022.105316

Bock, Y., Prawirodirdjo, L., Genrich, J. F., Stevens, C. W., McCaffrey, R., Subarya, C., Puntodewo, S. S. O., & Calais, E. (2003). Crustal Motion in Indonesia from Global Positioning System Measurements. *Journal of Geophysical Research: Solid Earth*, *108*(B8), 2001JB000324. https://doi.org/10.1029/2001JB000324

Carcole, E., & Sato, H. (2010). Spatial Distribution of Scattering Loss and Intrinsic Absorption of Short-Period *S* Waves in the Lithosphere of Japan on the Basis of the Multiple Lapse Time Window Analysis of Hi-Net Data. *Geophysical Journal International*, *180*(1), 268–290. https://doi.org/10.1111/j.1365-246X.2009.04394.x

Curray, J. R. (1989). The Sunda Arc: A Model for Oblique Plate Convergence. *Netherlands Journal of Sea Research*, *24*(2–3), 131–140. https://doi.org/10.1016/0077-7579(89)90144-0

Dasović, I., Herak, M., & Herak, D. (2012). Attenuation of Coda Waves in the Contact Zone between the Dinarides and the Adriatic Microplate. *Studia Geophysica et Geodaetica*, *56*(1), 231–247. https://doi.org/10.1007/s11200-010-0077-8

Filippucci, M., Lucente, S., Lorenzo, S. D., Pezzo, E. D., Prosser, G., & Tallarico, A. (2021). Seismic Envelopes of Coda Decay for Q-Coda Attenuation Studies of the Gargano Promontory (Southern Italy) and Surrounding Regions. *Data*, *6*(9), 98. https://doi.org/10.3390/data6090098

Havskov, J., Sørensen, M. B., Vales, D., Özyazıcıoğlu, M., Sánchez, G., & Li, B. (2016). Coda *Q* in Different Tectonic Areas, Influence of Processing Parameters. *Bulletin of the Seismological Society of America*, *106*(3), 956–970. https://doi.org/10.1785/0120150359

Hwang, H.-J., & Mitchell, B. J. (1987). Shear Velocities, Q, and the Frequency Dependence of Q in Stable and Tectonically Active Regions from Surface Wave Observations. *Geophysical Journal International*, *90*(3), 575–613. https://doi.org/10.1111/j.1365-246X.1987.tb00743.x

Jin, A., & Aki, K. (1988). Spatial and Temporal Correlation between Coda Q and Seismicity in China. *Bulletin of the Seismological Society of America*, *78*(2), 741–769. https://doi.org/10.1785/BSSA0780020741

Jin, A., & Aki, K. (1989). Spatial and Temporal Correlation between Coda Q^{-1} and Seismicity and Its Physical Mechanism. *Journal of Geophysical Research: Solid Earth*, *94*(B10), 14041–14059. https://doi.org/10.1029/JB094iB10p14041

Keep, M., Longley, I., & Jones, R. (2003). Sumba and Its Effect on Australia's Northwestern Margin. In R. R. Hillis & R. D. Müller, *Evolution and Dynamics of the Australian Plate*. Geological Society of America. https://doi.org/10.1130/0-8137-2372-8.309

Kumar, N., Parvez, I. A., & Virk, H. S. (2005). Estimation of Coda Wave Attenuation for NW Himalayan Region Using Local Earthquakes. *Physics of the Earth and Planetary Interiors*, *151*(3–4), 243–258. https://doi.org/10.1016/j.pepi.2005.03.010

Ma'hood, M., Hamzehloo, H., & Doloei, G. J. (2009). Attenuation of High Frequency P and S Waves in the Crust of the East-Central Iran. *Geophysical Journal International*, *179*(3), 1669–1678. https://doi.org/10.1111/j.1365-246X.2009.04363.x

Mak, S., Chan, L. S., Chandler, A. M., & Koo, R. C. H. (2004). Coda Q Estimates in the Hong Kong Region. *Journal of Asian Earth Sciences*, *24*(1), 127–136. https://doi.org/10.1016/j.jseaes.2003.10.001

McCaffrey, R. (2009). The Tectonic Framework of the Sumatran Subduction Zone. *Annual Review of Earth and Planetary Sciences*, *37*(1), 345–366. https://doi.org/10.1146/annurev.earth.031208.100212

Miller, M. S. (2019). *Transitions in the Banda Arc-Australia Continental Collision* [SEED Data]. International Federation of Digital Seismograph Networks. Retrieved from https://doi.org/10.7914/SN/YS_2014

Mitchell, B. J. (1995). Anelastic Structure and Evolution of the Continental Crust and Upper Mantle from Seismic Surface Wave Attenuation. *Reviews of Geophysics*, *33*(4), 441–462. https://doi.org/10.1029/95RG02074

Parvez, I. A., Sutar, A. K., Mridula, M., Mishra, S. K., & Rai, S. S. (2008). Coda Q Estimates in the Andaman Islands Using Local Earthquakes. *Pure and Applied Geophysics*, *165*(9–10), 1861–1878. https://doi.org/10.1007/s00024-008-0399-4

Pezzo, E. D. (2008). Chapter 13 Seismic Wave Scattering in Volcanoes. In *Advances in Geophysics* (Vol. 50, pp. 353–371). Elsevier. https://doi.org/10.1016/S0065-2687(08)00013-7

Priyono, A., Nugraha, A. D., Muzli, M., Ardianto, A., Aulia, A. N., Prabowo, B. S., Zulfakriza, Z., Rosalia, S., Sasmi, A. T., Afif, H., Sahara, D. P., Widiyantoro, S., Wei, S., Husni, Y. M., & Sarjan, A. F. N. (2021). Seismic Attenuation Tomography from 2018 Lombok Earthquakes, Indonesia. *Frontiers in Earth Science*, *9*, 639692. https://doi.org/10.3389/feart.2021.639692

Priyono, A., Suantika, G., Widiyantoro, S., & Nugraha, A. D. (2011). Three-Dimensional Seismic Attenuation Structure of Mt. Guntur, West Java, Indonesia. *International Journal of Tomography and Statistics*, *17*(S11), 17–28. Retrieved from https://www.researchgate.net/publication/285924219

Prudencio, J., Taira, T., Aoki, Y., Aoyama, H., & Onizawa, S. (2017). Intrinsic and Scattering Attenuation Images of Usu Volcano, Japan. *Bulletin of Volcanology*, *79*(4), 29. https://doi.org/10.1007/s00445-017-1117-9

Pulli, J. J. (1984). Attenuation of Coda Waves in New England. *Bulletin of the Seismological Society of America*, *74*(4), 1149–1166. https://doi.org/10.1785/BSSA0740041149

Rahimi, H., & Hamzehloo, H. (2008). Lapse Time and Frequency-Dependent Attenuation of Coda Waves in the Zagros Continental Collision Zone in Southwestern Iran. *Journal of Geophysics and Engineering*, *5*(2), 173–185. https://doi.org/10.1088/1742-2132/5/2/004

Rahimi, H., Motaghi, K., Mukhopadhyay, S., & Hamzehloo, H. (2010). Variation of Coda Wave Attenuation in the Alborz Region and Central Iran. *Geophysical Journal International*, *181*(3), 1643–1654. https://doi.org/10.1111/j.1365-246X.2010.04574.x

Roecker, S. W., Tucker, B., King, J., & Hatzfeld, D. (1982). Estimates of Q in Central Asia as a Function of Frequency and Depth Using the Coda of Locally Recorded Earthquakes. *Bulletin of the Seismological Society of America*, *72*(1), 129–149. https://doi.org/10.1785/BSSA0720010129

Sato, H. (1977). Energy Propagation Including Scattering Effects Single Isotropic Scattering Approximation. *Journal of Physics of the Earth*, *25*(1), 27–41. https://doi.org/10.4294/jpe1952.25.27

Sato, H., & Fehler, M. C. (1998). *Seismic Wave Propagation and Scattering in the Heterogeneous Earth*. New York: Springer. https://doi.org/10.1007/978-1-4612-2202-6

Sato, H., & Fehler, M. C. (2009). *Seismic Wave Propagation and Scattering in the Heterogeneous Earth*. Berlin Heidelberg: Springer. https://doi.org/10.1007/978-3-540-89623-4

Sharma, S., & Mitra, S. (2018). Seismic Attenuation of the Eastern Himalayan and Indo-Burman Plate Boundary Systems, Northeast India. *Journal of Geophysical Research: Solid Earth*, *123*(12). https://doi.org/10.1029/2018JB016496

Singh, D. D., Govoni, A., & Bragato, P. L. (2001). Coda Q Attenuation and Source Parameter Analysis in Friuli (NE Italy) and Its Vicinity. *Pure and Applied Geophysics*, *158*(9), 1737–1761. https://doi.org/10.1007/PL00022508

Singh, R., Sharma, S., Mitra, S., & Khan, P. K. (2019). Mapping of Coda-Wave Attenuation and Its Frequency Dependency Over Eastern Indian Shield. *Pure and Applied Geophysics*, *176*(12), 5291–5313. https://doi.org/10.1007/s00024-019-02284-3

Singh, S., & Herrmann, R. B. (1983). Regionalization of Crustal Coda *Q* in the Continental United States. *Journal of Geophysical Research: Solid Earth*, *88*(B1), 527–538. https://doi.org/10.1029/JB088iB01p00527

Sunarjo, S., Gunawan, M. T., & Pribadi, S. (2012). *Gempa Bumi* (Edisi Populer). Jakarta: Badan Meteorologi, Klimatologi, dan Geofisika.

Syuhada, S., Hananto, N. D., Abdullah, C. I., Puspito, N. T., Anggono, T., Febriani, F., & Soedjatmiko, B. (2020). Lithospheric Mantle Anisotropy from Local

Events Beneath the Sunda–Banda Arc Transition and Its Geodynamic Implications. *Acta Geophysica*, *68*(6), 1565–1593. https://doi.org/10.1007/s11600-020-00486-1

Syuhada, S., Hananto, N. D., Abdullah, C. I., Puspito, N. T., Anggono, T., & Yudistira, T. (2016). Crustal Structure Along Sunda-Banda Arc Transition Zone from Teleseismic Receiver Functions. *Acta Geophysica*, *64*(6), 2020–2049. https://doi.org/10.1515/acgeo-2015-0098

Talebi, A., Rahimi, H., & Moradi, A. (2024). Coda Wave Attenuation in the Zagros Collision Zone in Southwest of Iran and Its Tectonic Implications. *Acta Geophysica*, *73*(1), 119–130. https://doi.org/10.1007/s11600-024-01406-3

Wang, W., & Shearer, P. M. (2017). Using Direct and Coda Wave Envelopes to Resolve the Scattering and Intrinsic Attenuation Structure of Southern California. *Journal of Geophysical Research: Solid Earth*, *122*(9), 7236–7251. https://doi.org/10.1002/2016JB013810

Woodgold, C. R. D. (1994). Coda Q in the Charlevoix, Quebec, Region: Lapse-Time Dependence and Spatial and Temporal Comparisons. *Bulletin of the Seismological Society of America*, *84*(4), 1123–1131. https://doi.org/10.1785/BSSA0840041123

Wu, J., Jiao, W., Ming, Y., & Su, W. (2006). Attenuation of Coda Waves at the Changbaishan Tianchi Volcanic Area in Northeast China. *Pure and Applied Geophysics*, *163*(7), 1351–1368. https://doi.org/10.1007/s00024-006-0076-4

Zelt, B. C., Dotzev, N. T., Ellis, R. M., & Rogers, G. C. (1999). Coda *Q* in Southwestern British Columbia, Canada. *Bulletin of the Seismological Society of America*, *89*(4), 1083–1093. https://doi.org/10.1785/BSSA0890041083